

Communication

Generation of Ultrashort Pulses in XUV and X-ray FELs via an Excessive Reverse Undulator Taper

Evgeny Schneidmiller^{1,*}, Matthias Dreimann², Marion Kuhlmann¹, Juliane Rönsch-Schulenburg¹
and Helmut Zacharias²

¹ Deutsches Elektronen-Synchrotron DESY, Notkestr. 85, 22607 Hamburg, Germany

² Center for Soft Nanoscience, Westfälische Wilhelms-Universität, 48149 Münster, Germany

* Correspondence: evgeny.schneidmiller@desy.de

Abstract: The pulse duration in short-pulse schemes for Self-Amplified Spontaneous Emission Free Electron Lasers (SASE FELs) is limited by the FEL coherence time. A recently proposed concept allows to overcome the coherence time barrier and to obtain much shorter pulses. When the lasing part of an electron bunch is much shorter than the coherence time, one can suppress the radiation in the long main undulator while preserving microbunching within that short lasing slice. Then, a short radiation pulse is produced in a relatively short radiator. A possible suppression method, an excessive reverse undulator taper, is discussed and illustrated numerically in this paper. We also performed the first experimental tests of this method at the soft X-ray FEL user facility FLASH. The measured pulse duration approaches 1 fs (FWHM) at the wavelength of 5 nm.

Keywords: Free Electron Laser; SASE FEL; X-ray FEL; ultrashort pulses

1. Introduction

The possibility of generating few- and sub-femtosecond pulses in Extreme Ultraviolet (XUV) and X-ray FELs has been studied theoretically over past twenty years [1–7], and successful experimental demonstration of production of sub-femtosecond pulses was achieved recently [8–11]. Typically, the shortest pulse that can be generated in a SASE FEL is limited by FEL coherence time [12] which is given by the slippage of radiation with respect to electrons per FEL gain length.

A method to go beyond the coherence time limit in SASE FELs was proposed in [13]. One can create a short lasing slice within the electron bunch (much shorter than FEL coherence time). In the long main undulator, due to the SASE process, a microbunching (density modulation at the resonance wavelength) is generated within that short slice, but the radiation pulse is much longer (on the order of coherence time) due to the slippage in the undulator. At the second step, the modulated electron bunch produces a short radiation pulse in a short radiator, and the long radiation pulse from the main undulator is suppressed or separated from the short pulse (a similar concept was studied later in [14]). A specific way of selection of a short lasing slice, a laser manipulation of the electron bunch with the subsequent use of so-called chirp-taper scheme [6], was considered in [13]. However, the general principle can be used for different ways of creating a short lasing slice, which is also without a laser. Different methods of suppression (separation) were discussed in [13]; one of them is the application of an excessive reverse taper in the main undulator. In this communication, we discuss this method in more detail and illustrate it with numerical simulations for a short electron bunch, produced in the accelerator without the laser manipulation of its properties. We also present the first experimental results from XUV and soft X-ray FEL user facility FLASH [15].



Citation: Schneidmiller, E.; Dreimann, M.; Kuhlmann, M.; Rönsch-Schulenburg, J.; Zacharias, H. Generation of Ultrashort Pulses in XUV and X-ray FELs via an Excessive Reverse Undulator Taper. *Photonics* **2023**, *10*, 653. <https://doi.org/10.3390/photronics10060653>

Received: 28 April 2023

Revised: 26 May 2023

Accepted: 30 May 2023

Published: 5 June 2023



Copyright: © 2023 by the authors. Licensee MDPI, Basel, Switzerland. This article is an open access article distributed under the terms and conditions of the Creative Commons Attribution (CC BY) license (<https://creativecommons.org/licenses/by/4.0/>).

2. The Concept of Excessive Reverse Taper

To generate short X-ray pulses (much shorter than FEL coherence time) in a SASE FEL, one can make two steps:

- to generate a short electron bunch (or a short lasing part within longer bunch) and
- to apply a slippage-suppression mechanism in the undulator.

The latter can be realized in different ways proposed in [13]. In this paper, we consider one of them, reverse undulator taper (see Figure 1). The scheme is based on the effect discovered in [16]: in a reverse-tapered undulator the radiation power is strongly suppressed while bunching in the electron beam survives. Reverse taper means an increase of the undulator K value along the undulator length (this can be performed by reducing the gaps of undulator segments), in contrast to the standard sign of taper when the K decreases in order to maintain resonance after FEL saturation thus increasing radiation power. The reverse-taper concept was originally proposed in [16] for polarization control in X-ray FELs, and was used for this purpose at the Linac Coherent Light Source [17]. However, it has potentially broad applications such as background-free generation of harmonics in FELs [18], generation of coherent photons with orbital angular momentum [19], optimization of the performance of seeded FELs [20], etc.

A long electron bunch was considered in [16] but the concept also works for short bunches as will be illustrated numerically below in this paper. A short electron bunch propagates in a reverse-tapered main undulator where a strong microbunching is created but the radiation is very weak (and the radiation pulse is much longer than the modulated part of the electron bunch). Then, the bunch enters a short radiator, tuned to the resonance with the modulated beam, and produces a short (much shorter than FEL coherence time) and intense radiation pulse. An optimal number of periods in the undulator is approximately equal to the number of cycles in the microbunching. By a proper adjustment of parameters, the radiation background from the main undulator can be made negligible.

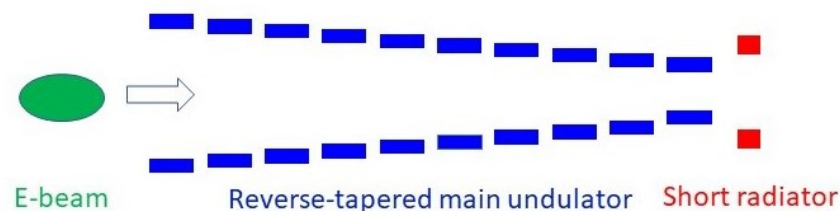


Figure 1. Conceptual scheme of ultrashort pulse production. A short electron bunch propagates in the reverse-tapered main undulator followed by a short radiator.

Short electron bunches can be generated in accelerator systems by a strong (linear or nonlinear) compression of initially long bunches. In case of nonlinear compression one typically obtains a short high-current leading peak (that is lasing) and a low-current long tail [8,15]. One can also use self-fields of the bunch to create high-current spikes in a dedicated chicane [9]. Alternatively, manipulations of long electron bunches with optical lasers, creating a lasing slice that is shorter than the laser wavelength, can be used. There are two most popular laser-based schemes: chirp-taper [6] and eSASE [5]. In the chirp-taper scheme, there is a short slice with the strong energy chirp being created by a laser beam in a short undulator. It was shown in [6] that a degrading effect of a linear energy chirp on SASE FEL gain can be compensated for by applying a linear undulator taper as soon as the following condition is satisfied:

$$\frac{dK}{dz} = \frac{(1 + K_0^2/2)^2}{K_0} \frac{1}{\gamma_0^3} \left(\frac{d\gamma}{ds} \right)_{in} \quad (1)$$

Here K_0 is the value of undulator parameter at the undulator entrance, $(d\gamma/ds)_{in}$ is the energy chirp at the undulator entrance, z is the coordinate along the undulator length, and

s is the coordinate along the bunch length. The compensation takes place within the slice with the strongest chirp. The rest of the bunch is unchirped (or weakly chirped) and suffers from a strong uncompensated taper, i.e., it practically does not lase.

In the eSASE scheme, the laser-induced energy modulation is converted into a density modulation in a chicane, so that a sharp current spike is created that lases most efficiently in the SASE undulator in a similar way as a short bunch generated without a laser. The energy chirp can be created by collective fields of the short bunch itself. The main effect is usually Longitudinal Space Charge (LSC) in the X-ray undulator. It scales there as $1/\gamma_z^2 = (1 + K^2/2)/\gamma^2$ [21], i.e., it can be much stronger than in a drift (where $K = 0$). When the chirp is mainly accumulated in the undulator and the bunch is sufficiently short, the linear taper in Equation (1) can be substituted by quadratic taper:

$$\frac{d^2K}{dz^2} = \frac{(1 + K_0^2/2)^2}{K_0} \frac{1}{\gamma_0^3} \frac{d^2\gamma}{dsdz} \tag{2}$$

with $d^2\gamma/dsdz$ being the rate of change of the energy slope $d\gamma/ds$ along the undulator length. When the energy chirp is accumulated inside and in front of the undulator, the tapering law for compensation can be described as follows:

$$K(z) = K_0 + \frac{dK}{dz}z + \frac{1}{2} \frac{d^2K}{dz^2}z^2 \tag{3}$$

with the derivatives from (1) and (2). Thus, for compensation of LSC-induced energy spread one can use both a reverse linear taper and a reverse quadratic taper. Of course, the LSC-induced chirp is nonlinear while the conditions (1) and (2) are valid for a linear chirp. It means that these conditions can provide only a partial compensation which might be sufficient in some practical situations. The LSC-induced chirp has a positive derivative $d\gamma/ds$ so that K must increase along the undulator length for compensation, i.e., one has to use a reverse taper.

For the purpose of the considered scheme, one should use a stronger reverse taper than that needed for chirp compensation, that is why we call the method “excessive reverse taper”. One can choose excessive linear or quadratic taper in order to suppress the radiation while keeping the strong bunching (more sophisticated taper laws can be considered as well). The proposed scheme works for chirped and unchirped bunches as will be illustrated in the next Section. The concept is easy to realize in practice since the undulator systems of X-ray FELs consist of relatively short segments. Thus, a reverse taper can be applied to a long string of segments while the last one can be used as a radiator. If it is too long, one can install a dedicated short radiator.

3. Numerical Example

We illustrate the concept of excessive reverse taper with the parameters of FLASH2 undulator of FEL user facility FLASH, see detailed description in the next Section. The variable-gap undulator consists of twelve segments, each of them has a period of 3.14 cm and is 2.5 m long. We consider an electron beam with the following parameters: energy is 1.2 GeV, rms bunch duration is 1 fs, peak current is 2 kA, rms normalized emittance is 0.8 mm mrad, and rms uncorrelated energy spread is 300 keV. The average beta-function in the undulator is 7 m. FEL wavelength is 5 nm which corresponds to $K = 1.24$. The FEL simulations are performed with the code SIMPLEX [22].

First, we simulate standard SASE regime and ignore LSC effects. The number of undulator segments is 9, and the amplification process is stopped at the onset of saturation. If the undulator is longer, the radiation pulses are becoming longer too, but the peak power does not increase. Three typical shots are presented on Figure 2 (upper plot), as three color lines, typical pulse duration is 3 fs (FWHM). The current distribution $I(t)$ is shown with dashed line while the solid black line represents the function $[I(t)|b(t)]^2$ with $b(t)$ being the bunching factor [12] for a typical shot. If the bunching factor is real, the function

$[I(t)|b(t)]^2$ gives a radiation power profile from a short radiator. One can notice that the radiation pulses on Figure 2 (upper plot) are essentially longer due to the slippage in the last part of the undulator.

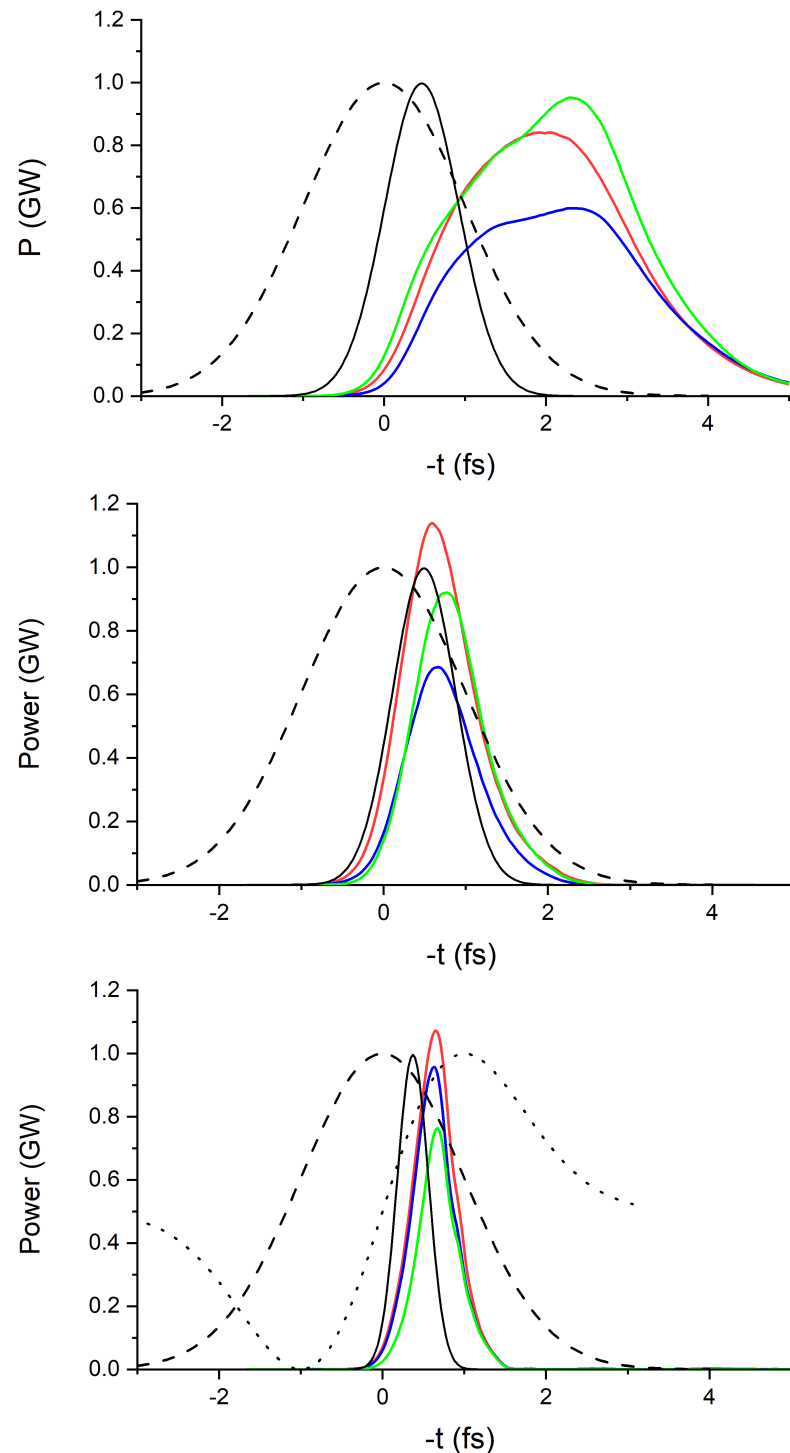


Figure 2. Typical radiation pulses (color lines) for three different configurations: standard SASE, no LSC (**upper plot**), reverse linear taper in the main undulator plus short radiator, no LSC (**middle plot**), and excessive reverse quadratic taper in the main undulator plus short radiator, LSC in the undulator included (**lower plot**). Black dashed lines represent the current profile $I(t)$ (bunch head is on the right), black solid lines show the product $[I(t)|b(t)]^2$ for a typical shot, dotted line on the lower plot shows the shape of LSC-wake. All black curves are presented in arbitrary units for a vertical scale, the color curves show radiation power in gigawatts.

Second, we simulate the reverse-tapered configuration, assuming again no energy chirp due to LSC. We use eleven undulator segments and apply the linear reverse taper with the strength $dK/dz = 1.5 \times 10^{-3} \text{ m}^{-1}$ to obtain a strong bunching ($\approx 0.4\text{--}0.5$) while suppressing the radiation in this undulator. The radiator has the same period as segments of the main undulator but the number of periods is reduced to 50, the value of K is optimized at 1.243. We also focus the electron beam stronger in the radiator, the beta-function is 2 m. This helps us to increase the radiation power and improve the contrast of short pulses. The results of numerical simulations are shown on Figure 2 (middle plot). Three typical shots are shown as color plots, the pulse duration is now about 1 fs. The function $[I(t)|b(t)]^2$ has a narrower width than that for the standard SASE regime shown on the upper plot, thus we can conclude that the excessive reverse taper effectively reduces the width of generated bunching distribution.

Third, we include the LSC-induced energy chirp [21] in the undulator in our simulations. The shape of LSC-wake is shown in Figure 2 (lower plot), it has zero crossing at the location of the maximum current (note that the dotted line is shifted vertically). At the end of the undulator the peak-to-peak energy deviation is about 12 MeV. The main undulator consists of eleven segments, we apply the excessive reverse quadratic taper $d^2K/dz^2 = 5.5 \times 10^{-4} \text{ m}^{-2}$. The number of periods in the radiator is 50, K equals 1.39, beta-function is 2 m. From Figure 2 (lower plot) one can see that the width of the function $[I(t)|b(t)]^2$ is reduced further, this is the consequence of nonlinear energy chirp [23] and excessive reverse taper. Radiation pulses have average duration of 0.6 fs.

We can conclude that our concept (excessive reverse taper in the main undulator plus a short radiator) works well with and without energy chirp, but a strong chirp helps further reduce pulse duration. In principle, the reduction of pulse duration with respect to a standard SASE case can be much stronger than in the considered numerical example provided that one can generate ultrashort electron bunches (or their lasing parts). In other words, there is no conceptual lower limit for FEL pulse duration except the applicability of the standard FEL theory (a pulse must contain many cycles [12]).

4. Experiment at FLASH

FLASH [15] is the first free-electron laser for XUV and soft X-ray radiation. It covers a wavelength range from 4 nm to about 90 nm with GW peak power and pulse durations between a few fs and 200 fs. The electron bunches with maximum energy of 1.35 GeV are distributed between the two branches, FLASH1 and FLASH2 [24], see Figure 3. The facility is based on the superconducting accelerator which allows to operate in a “burst mode” with long pulse trains (several hundred pulses) at 10 Hz repetition rate. Presently, the facility is being upgraded towards high repetition rate seeding in the FLASH1 branch [25]. The segmented variable-gap undulator of FLASH2 has a period of 3.14 cm and can provide a maximum undulator parameter K about 2.7. FLASH2 hosts twelve 2.5 m long segments with quadrupoles in the intersections.

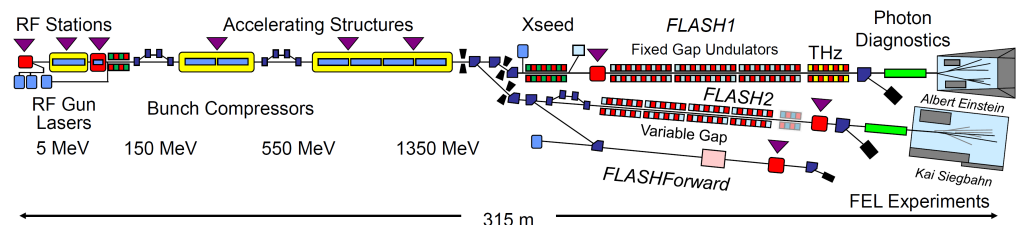


Figure 3. FLASH layout.

Electron bunches for FLASH2 are produced in the photoinjector and then longitudinally compressed in three bunch compressors at different electron energies. The last compressor is placed in front of the undulator and the compression takes place at the final beam energy. This simplifies the task of formation of short high-current bunches because

the impact of collective effects such as coherent synchrotron radiation and space charge on a quality of short electron bunches are reduced with respect to a final compression at lower energies. Nevertheless, the LSC effect can still be significant as soon as the bunches are strongly compressed.

The experiment was performed in March 2023. The electron energy was 1.2 GeV, the FEL wavelength was 5 nm, undulator K was 1.24. We used a photoinjector laser with 1 ps duration to generate an electron bunch with a charge of 80 pC. We performed nonlinear compression [15] in order to generate a short high-current leading peak for production of short radiation pulses. Diagnostics to characterize the electron beam properties is only partially available during parallel operation of the two branches of FLASH, and it was not possible for us to measure relevant properties of the bunch (such as emittance, etc.).

We used the standard photon diagnostics including the Gas Monitor Detector (GMD) [26] to measure an absolute pulse energy, and the grating spectrometer [27] to measure single-shot spectra. Beamline transmission to the spectrometer at 5 nm was about 5.5×10^{-4} . However, we could clearly distinguish between single- and multi-mode operation of SASE FEL; the resolution was sufficient for this purpose.

First, we established a standard single-spike (or single mode [12]) operation of SASE FEL. Reverse linear taper with the strength $dK/dz = 4.5 \times 10^{-4} \text{ m}^{-1}$ was used to compensate for energy chirp [6] induced by the LSC across a short lasing peak in electron density distribution. Single-shot spectra, corresponding to this regime, are presented in Figure 4. Most of the observed spectra were single-spike events with a rare appearance of two spikes. At the next step we set up the undulator in a way described above in this paper: excessive reverse taper plus a short radiator. The undulator configuration was as follows: eleven segments were linearly reverse-tapered with the strength $dK/dz = 2 \times 10^{-3} \text{ m}^{-1}$. The 12th undulator segment played the role of the radiator, the value of K was 1.265. In order to effectively reduce the length of this radiator, we used an ambient field correction coil to turn the beam inside that segment, and then we used an iris to cut a part of the photon beam that was horizontally streaked. The average pulse energy in this configuration was 1.5 μJ during the measurement.

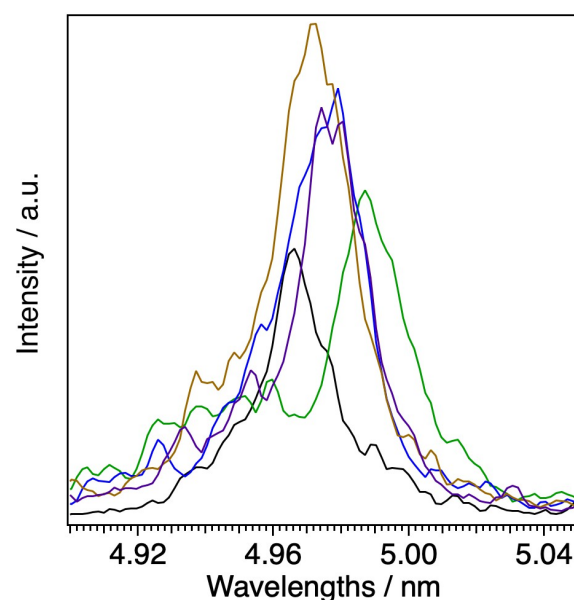


Figure 4. Representative set of single-shot spectra for FEL operation in the standard SASE regime.

To measure the pulse duration, we used the autocorrelation method. The split-and-delay unit [28] with the time resolution of 120 as was used. It splitted spatially the incoming FEL beam into two partial beams. Both beams were overlapped at a crossing angle of 40 μrad at a distance of 24 m to the last mirror of the SDU on a UHV compatible CCD

camera. From the observed interference fringes the visibility V was evaluated. For every delay step, 25 shots were taken and the visibility averaged. The standard deviation is derived from 25 single shot visibility measurements, and amounts to an average ΔV of ± 0.01 with values up to $\Delta V = \pm 0.08$. By scanning the delay and measuring the visibility of fringes, we can measure the field autocorrelation:

$$A(\tau) \propto \int_{-\infty}^{\infty} E(t)E^*(t - \tau)dt \tag{4}$$

where $E(t)$ is the complex amplitude of the electric field. More precisely, we measure the ensemble-averaged modulus of the field autocorrelation.

The measured autocorrelation trace is shown in Figure 5. The full width at half maximum (FWHM) of this trace is 1.88 ± 0.21 fs.

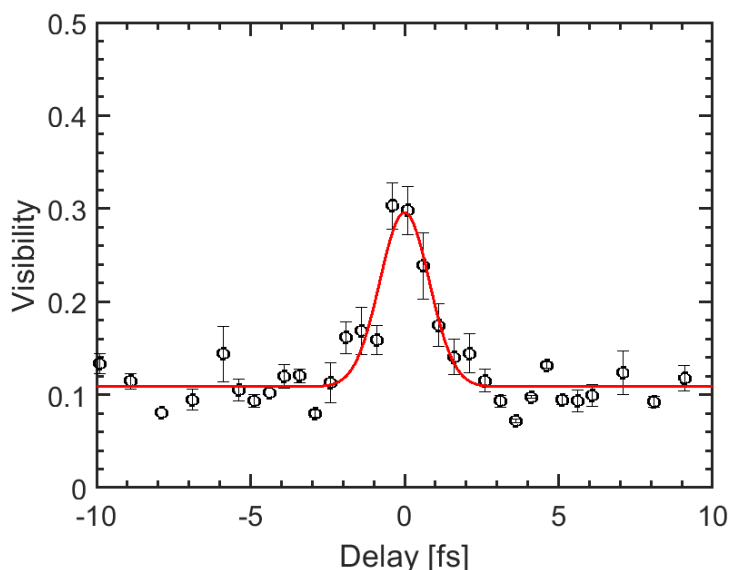


Figure 5. Field autocorrelation trace (measurement).

The next task is to estimate pulse duration from this measurement. For a Gaussian laser pulse without a frequency chirp, the relation between the FWHM of the intensity distribution τ_I^{FWHM} and the FWHM of the field autocorrelation τ_{AC}^{FWHM} is given by a simple relation:

$$\tau_I^{FWHM} = 0.5\tau_{AC}^{FWHM} \tag{5}$$

Our pulses are, in general, non-Gaussian and they can have frequency chirps. To estimate the pulses duration from autocorrelation measurement we can use the coefficient found in numerical simulations. We ran simulations of the considered scheme with different parameters of electron bunch resulted in different energy chirps, and we also considered the case with no chirp. We compared the average pulse duration and the width of the average autocorrelation function in those simulations. We found that instead of factor 0.5 in Equation (5) we should use the factor 0.67 ± 0.12 , i.e.,

$$\tau_I^{FWHM} = 0.67\tau_{AC}^{FWHM} \tag{6}$$

Thus, to our best knowledge, we can estimate the pulse duration in this experiment at $\tau_I^{FWHM} = 1.26 \pm 0.37$ fs.

5. Discussion

In this communication, we demonstrated in numerical simulations the validity of previously proposed method [13] of generation of short pulses in SASE FELs, namely, excessive reverse taper in the main undulator in combination with a short radiator. More-

over, we performed the experiment at the soft X-ray FEL user facility FLASH and obtained record short pulses for this facility using the proposed undulator configuration. Despite a relatively low intensity, such pulses are of great interest for the FLASH user community. In particular, in most of the experiments on solids, the photon beam is attenuated to the level below 1 μJ . Pulses at this intensity level having 1 fs duration promise an excellent temporal resolution. Moreover, by an appropriate focusing of the beam on a sample one can reach intensity level 10^{16} W/cm^2 and study nonlinear effects. In the future, we plan to reduce the bunch charge further and to try nonlinear as well as linear compression, and to operate at a higher electron energy and a shorter wavelength (below 4 nm) in order to be able to produce sub-femtosecond pulses at FLASH. With several thousand pulses per second this can be a unique source for attosecond science. Application of the proposed technique to hard X-ray FELs can open the way to generate extremely short pulses (in the regime of few tens attoseconds) as suggested in [13].

Author Contributions: Conceptualization, E.S.; methodology, E.S.; software, M.D.; validation, E.S. and M.D.; formal analysis, E.S.; investigation, E.S., M.D., M.K., J.R.-S. and H.Z.; resources, M.D., M.K. and H.Z.; data curation, E.S., M.D., H.Z. and M.K.; writing—original draft preparation, E.S.; writing—review and editing, E.S. All authors have read and agreed to the published version of the manuscript.

Funding: HZ gratefully acknowledges partial funding via BMBF project 05K19PM1.

Institutional Review Board Statement: Not applicable.

Informed Consent Statement: Not applicable.

Acknowledgments: We would like to thank scientific and technical staff of FLASH for support. We are grateful to L. Schaper for careful reading of the manuscript and useful suggestions, and to W. Leemans for his interest in this work. We thank M. Guehr and M. Beye for fruitful discussions on possible applications of short pulses at FLASH.

Conflicts of Interest: The authors declare no conflict of interest.

References

1. Saldin, E.L.; Schneidmiller, E.A.; Yurkov, M.V. Scheme for attophysics experiments at a X-ray SASE FEL. *Opt. Commun.* **2002**, *212*, 377–390. [CrossRef]
2. Saldin, E.L.; Schneidmiller, E.A.; Yurkov, M.V. Terawatt-scale sub-10-fs laser technology—key to generation of GW-level attosecond pulses in X-ray free electron laser. *Opt. Commun.* **2004**, *237*, 153–164. [CrossRef]
3. Zholents, A.A.; Fawley, W.M. Proposal for intense attosecond radiation from an X-ray free-electron laser. *Phys. Rev. Lett.* **2004**, *92*, 224801. [CrossRef] [PubMed]
4. Emma, P.; Huang, Z.; Borland, M. Proc. of the FEL2004 Conference, p. 333. Available online: <http://www.jacow.org> (accessed on 26 May 2023).
5. Zholents, A.A.; Penn, G. Obtaining attosecond x-ray pulses using a self-amplified spontaneous emission free electron laser. *Phys. Rev. Spec.-Top. Beams* **2005**, *8*, 050704. [CrossRef]
6. Saldin, E.L.; Schneidmiller, E.A.; Yurkov, M.V. Self-amplified spontaneous emission FEL with energy-chirped electron beam and its application for generation of attosecond X-ray pulses. *Phys. Rev. Spec.-Top. Beams* **2006**, *9*, 050702. [CrossRef]
7. Ding, Y.; Huang, Z.; Ratner, D.; Bucksbaum, P.; Merdji, H. Generation of attosecond x-ray pulses with a multicycle two-color enhanced self-amplified spontaneous emission scheme. *Phys. Rev. Spec.-Top. Beams* **2009**, *12*, 060703. [CrossRef]
8. Huang, S.; Ding, Y.; Feng, Y.; Hemsing, E.; Huang, Z.; Krzywinski, J.; Lutman, A.A.; Marinelli, A.; Maxwell, T.J.; Zhu, D. Generating single-spike hard X-ray pulses with nonlinear bunch compression in free-electron lasers. *Phys. Rev. Lett.* **2017**, *119*, 154801. [CrossRef]
9. Duris, J.; Li, S.; Driver, T.; Champenois, E.G.; MacArthur, J.P.; Lutman, A.A.; Zhang, Z.; Rosenberger, P.; Aldrich, J.W.; Coffee, R.; et al. Tunable isolated attosecond X-ray pulses with gigawatt peak power from a free-electron laser. *Nat. Photonics* **2020**, *14*, 30–36. [CrossRef]
10. Malyzhenkov, A.; Arbelo, Y.P.; Craievich, P.; Dijkstal, P.; Ferrari, E.; Reiche, S.; Schietinger, T.; Juranić, P.; Prat, E. Single- and two-color attosecond hard x-ray free-electron laser pulses with nonlinear compression. *Phys. Rev. Res.* **2020**, *2*, 042018(R). [CrossRef]
11. Trebushinin, A.; Geloni, G.; Serkez, S.; Mercurio, G.; Gerasimova, N.; Maltezopoulos, T.; Guetg, M.; Schneidmiller, E. Experimental Demonstration of Attoseconds-at-Harmonics at the SASE3 Undulator of the European XFEL. *Photonics* **2023**, *10*, 131. [CrossRef]
12. Saldin, E.L.; Schneidmiller, E.A.; Yurkov, M.V. *The Physics of Free Electron Lasers*; Springer: Berlin/Heidelberg, Germany, 1999.

13. Schneidmiller, E.A. Application of a modified chirp-taper scheme for generation of attosecond pulses in extreme ultraviolet and soft X-ray free electron lasers. *Phys. Rev. Accel. Beams* **2022**, *25*, 010701. [[CrossRef](#)]
14. Tu, L.; Qi, Z.; Wang, Z.; Zhao, S.; Lu, Y.; Fan, W.; Sun, H.; Wang, X.; Feng, C.; Zhao, Z. Improving the Performance of an Ultrashort Soft X-ray Free-Electron Laser via Attosecond Afterburners. *Appl. Sci.* **2022**, *12*, 11850. [[CrossRef](#)]
15. Ackermann, W.A.; Asova, G.; Ayvazyan, V.; Azima, A.; Baboi, N.; Bähr, J.; Balandin, V.; Beutner, B.; Brandt, A.; Bolzmann, A.; et al. Operation of a free-electron laser from the extreme ultraviolet to the water window. *Nat. Photonics* **2007**, *1*, 336–342. [[CrossRef](#)]
16. Schneidmiller, E.A.; Yurkov, M.V. Obtaining high degree of circular polarization at x-ray free electron lasers via a reverse undulator taper. *Phys. Rev. Spec.-Top. Beams* **2013**, *16*, 110702. [[CrossRef](#)]
17. Lutman, A.A.; MacArthur, J.P.; Ilchen, M.; Lindahl, A.O.; Buck, J.; Coffee, R.N.; Dakovski, G.L.; Dammann, L.; Ding, Y.; Dürr, H.A.; et al. Polarization control in an X-ray free-electron laser. *Nat. Photonics* **2016**, *10*, 468–472. [[CrossRef](#)]
18. Schneidmiller, E.A.; Yurkov, M.V. Reverse undulator tapering for polarization control and background-free Harmonic production in XFELS: Results From Flash. In Proceedings of the 38th International Free Electron Laser Conference FEL2017, 20–25 August 2017, Santa Fe, NM, USA; JACoW Publishing: Geneva, Switzerland, 2017; p. 106. ISBN 978-3-95450-179-3. [[CrossRef](#)]
19. Hensing, E. Coherent photons with angular momentum in a helical afterburner. *Phys. Rev. Accel. Beams* **2020**, *23*, 020703. [[CrossRef](#)]
20. Zhang, K.; Liu, T.; Qi, Z.; Fu, X.; Feng, C.; Deng, H.; Liu, B. Extending the Photon Energy Coverage of a Seeded Free-Electron Laser via Reverse Taper Enhanced Harmonic Cascade. *Photonics* **2021**, *8*, 44 [[CrossRef](#)]
21. Geloni, G.; Saldin, E.; Schneidmiller, E.; Yurkov, M. Scheme for stabilization of output power of an X-ray self-amplified spontaneous emission free-electron laser. *Nucl. Instr. Methods* **2007**, *A583*, 228. [[CrossRef](#)]
22. Tanaka, T. SIMPLEX: Simulator and postprocessor for free-electron laser experiments. *J. Synchrotron Radiat.* **2015**, *22*, 1319–1326. [[CrossRef](#)]
23. Baxevanis, P.; Duris, J.; Huang, Z.; Marinelli, A. Time-domain analysis of attosecond pulse generation in an X-ray free-electron laser. *Phys. Rev. Accel. Beams* **2018**, *21*, 110702. [[CrossRef](#)]
24. Faatz, B.; Plönjes, E.; Ackermann, S.; Agababyan, A.; Asgekar, V.; Ayvazyan, V.; Baark, S.; Baboi, N.; Balin, V.; Von Bargen, N.; et al. Simultaneous operation of two soft x-ray free-electron lasers driven by one linear accelerator. *New J. Phys.* **2016**, *18*, 062002. [[CrossRef](#)]
25. Schaper, L.; Ackermann, S.; Allaria, E.; Amstutz, P.; Baev, K.; Beye, M.; Gerth, C.; Hartl, I.; Hillert, W.; Honkavaara, K.; et al. Flexible and Coherent Soft X-ray Pulses at High Repetition Rate: Current Research and Perspectives. *Appl. Sci.* **2021**, *11*, 9729. [[CrossRef](#)]
26. Sorokin, A.A.; Bican, Y.; Bonfigt, S.; Brachmanski, M.; Braune, M.; Jastrow, U.F.; Gottwald, A.; Kaser, H.; Richter, M.; Tiedtke, K. An X-ray gas monitor for free-electron lasers. *J. Synchrotron Rad.* **2019**, *26*, 1092–1100. [[CrossRef](#)] [[PubMed](#)]
27. Tanikawa, T.; Hage, A.; Kuhlmann, M.; Gonschior, J.; Grunewald, S.; Plönjes, E.; Düsterer, S.; Brenner, G.; Dziarzhytski, S.; Braune, M.; et al. First observation of SASE radiation using the compact wide-spectral-range XUV spectrometer at FLASH2. *Nucl. Instrum. Methods Phys. Res. Sect. A Accel. Spectrometers Detect. Assoc. Equip.* **2016**, *830*, 170–175. [[CrossRef](#)]
28. Dreimann, M.; Wahlert, F.; Eckermann, D.; Rosenthal, F.; Roling, S.; Reiker, T.; Kuhlmann, M.; Toleikis, S.; Brachmanski, M.; Treusch, R.; et al. The soft X-ray and XUV split-and-delay unit at beamlines FL23/24 at FLASH2. *J. Synchrotron Radiat.* **2023**, *30*, 479. [[CrossRef](#)]

Disclaimer/Publisher’s Note: The statements, opinions and data contained in all publications are solely those of the individual author(s) and contributor(s) and not of MDPI and/or the editor(s). MDPI and/or the editor(s) disclaim responsibility for any injury to people or property resulting from any ideas, methods, instructions or products referred to in the content.